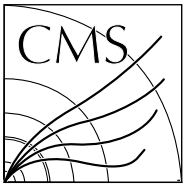

The Compact Muon Solenoid Experiment

**CMS Note**

Mailing address: CMS CERN, CH-1211 GENEVA 23, Switzerland

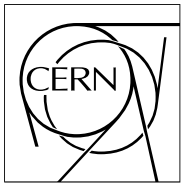

**June 10, 2006**

# Search for SUSY in top final states in the mSUGRA scenario at CMS

S. Paktinat Mehdiabadi[a]

*Institute for Studies in Theoretical Physics & Mathematics (IPM), Tehran, Iran*

L. Pape

*ETH, Zurich, Switzerland*

M. Spiropulu

*CERN, Geneva, Switzerland*

**Abstract**

A search for SUSY is performed in a low mass mSUGRA test point by looking for top quark enriched in the final states. A robust algorithm is developed to suppress the electrons faking a jet and a two constraints kinematic fit is utilized to improve the top quark extraction. It is found that the signal over background ratio is 11.0 and a 5 $\sigma$ excess can be observed with 0.2 $fb^{-1}$. The fast simulation of the detector response is used to find the CMS potential discovery for SUSY in this channel. The reach contours for 1, 10 and 30 $fb^{-1}$ are presented.

a) Also at *Sharif University of Technology, Tehran, Iran*

# 1 Introduction

Supersymmetric scenarios [1] provide a very promising extension for the standard model (SM) solving the quadratic divergencies and hierarchy problem. Supersymmetry imposes a new symmetry between the fermionic and bosonic degrees of freedom. In this analysis we focus on mSUGRA, where gravity is responsible for soft supersymmetry breaking. Top can be generated inclusively from the decay of heavy squarks or gluinos accompanied by a neutralino. This neutralino can be either the lightest supersymmetric particle (LSP) or a heavier neutralino that decays inclusively and ends up to a LSP that is a stable particle (assuming R-parity conservation) and appears as missing transverse energy (MET). Hence in the final state there is at least a top quark plus a large MET. The approach is to use this feature to look for an excess in the number of the extracted top quarks in the tail of the MET distribution from the $t\bar{t}$ events. The analysis is optimized to have a pure sample as signal. It would be very useful in future analysis where one needs to use the extracted top quark to reconstruct the kinematic features of the involved sparticles. A robust method is used to avoid double-counting the energy of electrons as jets and a two-constraint kinematic fit is utilized to extract the top quark.

The structure of this note is as follows: in section 2 the used sample in the kinematic fit and the reconstruction algorithms for jets and leptons are explained. Section 3 is devoted to kinematic fit and top extraction. In section 4, the production and decay of the related sparticles is reviewed, in section 5, the simulated samples for the SUSY search are described, section 6 describes what cuts are used to enhance the signal against the background, systematic uncertainties are discussed in section 7, final results of the full simulation are reported in section 8, section 9 is devoted to describe the search strategy to find the CMS reach in this channel and section 10 concludes the note.

# 2 The Data Samples and Reconstruction Algorithms

The main sample (referred to as LM1-stop sample) used to study the kinematic fit in section 3 was produced for the scalar top quark search in point CMS-LM1 (mSUGRA scenario, $m_0$ = 60 GeV, $m_{1/2}$ = 250, tan($\beta$) = 10, $A_0$ = 0 and $\mu > 0$, point $B^{'}$ [2]). Every event is required to have at least one scalar top quark that decays as follows:

$$\tilde{t_1} \rightarrow t + \chi_2^0 \rightarrow t + \tilde{l}_R + l \rightarrow t + l + l + \chi_1^0 \tag{1}$$

The $\tilde{t_1}$ is produced inclusively. The sample that contains 7120 events was generated using the ISAJET 7.69 [3] interfaced with PYTHIA 6.225 [4] within the CMKIN 4_0_0 [5] package. The events were simulated using the detailed simulation of CMS, OSCAR_3_6_0 [6], digitized with low luminosity pileup and reconstructed with the CMS reconstruction package, ORCA_8_7_1 [7].

## 2.1 Muon reconstruction and selection

The muons in this analysis are reconstructed using the global information from the muon system, calorimeters and tracker [8]. In the following, the minimum $P_T$ requirement of the leptons used in this analysis is 5 GeV/$c$ for both muons and electrons. All leptons must be within $|\eta| \leq 2.5$.

The number of hits that is used to reconstruct a muon is chosen as a good muon identification variable (Fig. 1). A reconstructed lepton (muon or electron) is defined as "matched" if and only if there is a generated lepton (with the same flavour) from a hard process within $\Delta R = \sqrt{(\Delta\eta)^2 + (\Delta\phi)^2} < 0.03$. To increase the ratio of matched muons over the unmatched ones, at least 20 hits are required in a reconstructed muon. The efficiencies of this requirement are 91% and 86% for matched and all muons, respectively.

## 2.2 Electron reconstruction and selection

To reconstruct the electrons the information of the electromagnetic calorimeter (ECAL) and fully reconstructed tracks are combined [8]. The energy deposit in the electromagnetic calorimeter is assigned to the direction of the associated track, it will recover mostly the bremsstrahlung radiation. To clean up the sample before applying isolation criteria, the following electron-id requirements (discussed also in [9]) are used.

**HoE :** ratio of the energy deposited in the hadronic calorimeter (HCAL) tower behind the most energetic cluster of the ECAL over the energy of the electron in ECAL;

$\Delta\eta$ **:** absolute difference between the measured $\eta$ in the calorimeter and the $\eta$ of the associated track;

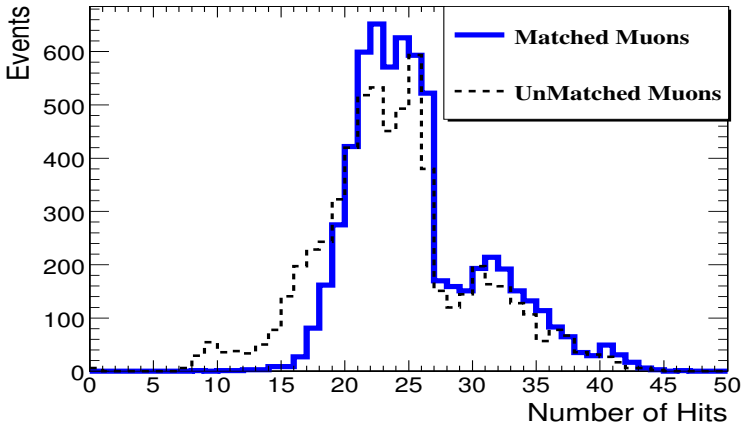


Figure 1: The number of hits used to reconstruct a muon (in LM1-stop sample). To compare the shapes, the two histograms are normalized to have the same number of entries.

**$\eta$ spread ($\sigma_{\eta\eta}$):** energy weighted spread of the electron's shower in $\eta$ direction;

These variables are accessible directly from the reconstructed electron in ORCA [7]. Figure 2 shows the distribu-

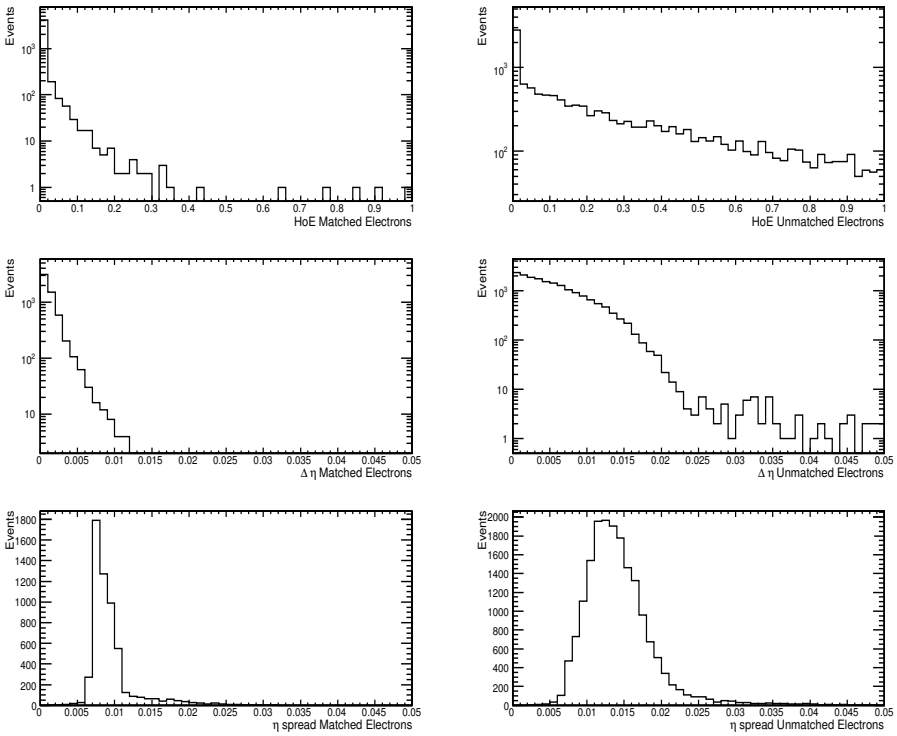


Figure 2: Distribution of electron-id variables (in LM1-stop sample) used for matched (left) and unmatched (right) electrons. From top, HoE, $\Delta\eta$ and $\eta$ shower spread are shown.

tions of these variables for both matched and unmatched electrons. The requirements imposed are:

- $HoE \leq 0.1$
- $\Delta\eta \leq 0.006$
- $\sigma_{\eta\eta} \leq 0.015$

The efficiencies inside acceptance for the requirements on these $P_T$ independent [9] variables are shown in Table 1. The purity is defined as the fraction of all reconstructed electrons that are matched.

Table 1: Electron-id requirements and their efficiency for all electrons. The number of the matched electrons and the purity also is shown. The first line shows the number of electrons before any requirement and the last line shows the overall efficiency of the cuts.

| variable | cut | No.Ele | Eff | No.Matched | purity |
|---|---|---|---|---|---|
| | No cut | 23885 | — | 5657 | 23.7% |
| HoE | 0.1 | 11625 | 48.6% | 5561 | 47.8% |
| $\Delta\eta$ | 0.006 | 9446 | 81.3% | 5498 | 58.2% |
| $\eta$ spread | 0.015 | 8200 | 86.8% | 5147 | 62.8% |
| | All cuts | 8200 | 34.3% | 5147 | 62.8% |

Apart from the mentioned cuts, leptons are required to be isolated, namely that the ratio of $P_T$ of the lepton to the sum of $P_T$ of other tracks inside a cone of size $\Delta R = 0.1$ around the lepton track be greater than 2.

### 2.3 Jet and MET reconstruction and selection

Jets were reconstructed from ECAL and HCAL towers by the iterative cone algorithm with cone size $\Delta R = 0.5$. Those towers that contain energy from an isolated electron are rejected from the list of input towers used in the jet clustering. Jets are calibrated using corrections from photon-jet balancing studies [10]. Calibrated jets with $E_T \geq 30$ GeV and $|\eta| \leq 2.5$ that before calibration have $E_T \geq 20$ GeV are considered. The b-tagging is done using an impact parameter algorithm as implemented in `TrackCountingBTagging` [8]. MET was reconstructed from the vector sum of the ECAL and HCAL towers. It is corrected for the identified muons.

## 3 2C Kinematic Fit for Top Quark Extraction

Extracting the top quark in a multi-jets environment requires eliminating the huge combinatorial background which can easily hide the signal. In order to select the real combination of the jets originated from a top quark, we utilize a kinematic fit with constraints.

Since the purpose of the study is not to measure the mass of the top quark, its mass is used as a constraint, so in a hadronic decay of a top quark the two main constraints are:

**W mass:** The invariant mass of two non b-tagged jets must be equal to the known mass of the W boson.

**Top mass:** The invariant mass of these two jets and a b-tagged jet must be equal to the mass of the top quark.

A similar method has been used in ATLAS to reconstruct the fully hadronic decay of the $t\bar{t}$ [11]. There, the W mass constraint is used to find two distinct W's and the best W candidates are selected by a $\chi^2$ cut. The second constraint is that in every event the mass of $t$ and $\bar{t}$ must be equal and is applied to find the best b-jets. Here an alternative algorithm, based on a kinematic fit of the jet energies using both constraints simultaneously, is developed and used. Jet angles are not varied in the fit.

It is based on the minimization of a $\chi^2$ in which the constraints are taken into account by the Lagrange multipliers, originally introduced in [12]. After linearization of the problem, the solution is computed iteratively by inversion of a matrix. This inversion is simplified by using the fact that the matrix contains blocks of zeros and can be reduced to operations on smaller matrices, a method called "Partitioned Matrix Method". Details of the mathematical framework of a more generic procedure and some examples can be found in Reference [13].

All plots and numbers in this section refer to the LM1-stop sample, unless it is expressed explicitly.

### 3.1 Results for top quark extraction

In every event different combinations are fitted and the minimum $\chi^2$ for every combination is found. Each combination contains two non b-tagged jets and one b-tagged jet. We use the jet resolution parametrization, reported in Reference [14]. The parametrization was done for MC calibrated jets in a sample of the $2 \rightarrow 2$ jets events. If

the fit converges, the combination with the least $\chi^2$ is selected as the right combination. Figure 3 shows different distributions for these selected combinations. In the following figures and tables this kinematic fitting algorithm is referred to as 'Partitioned Matrix'. The $\chi^2$ probability distribution in figure 3 (top-right), has a peak in the

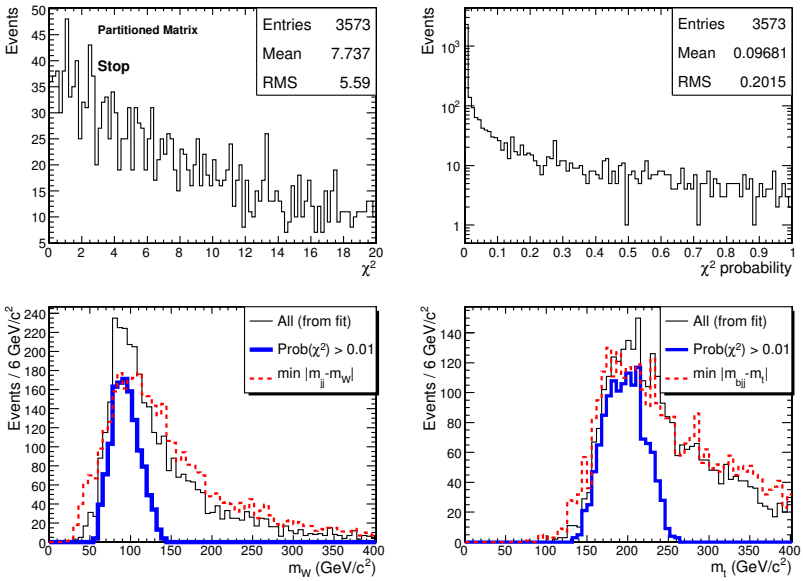


Figure 3: The distribution of the least $\chi^2$ solution in every event (top-left) and distribution of its probability (top-right). The dijet and bjj invariant masses for the least $\chi^2$ are shown in the second row. The fit results with (thick blue) and without (narrow black) the cut on the $\chi^2$ probability are compared with the results from a test algorithm (dotted red) explained in the text. The fit gives a narrower distribution with controllable tails.

low probability region. These events have a large $\chi^2$ either because the tested hypothesis is wrong or because the uncertainty on the jet resolution used in the fit is not correctly estimated. To remove the effect of these low probability events, a cut on the $\chi^2$ probability is introduced and combinations with a $\chi^2$ probability less than 0.01 ($\chi^2 > 9.2$) are rejected. The W, and top quark invariant mass distributions after applying the cut are shown in figure 3 (bottom) with thick (blue) lines. This cut mostly removes combinations in the tails of the mass distribution of the W and the top.

To evaluate the performance of the fit, a test algorithm is used to extract the top quark. In this algorithm the di-jet with the closest invariant mass to $M_W = 80$ GeV is used as the W candidate and a b-jet that minimizes $|m_{bjj} - 175|$ is used to extract the hadronically decaying top quark candidates. The corresponding distributions for this algorithm are shown with the dotted (red) lines in figure 3 (bottom). When using the fit the width of the distributions is smaller.

Table 2 compares different algorithms of top extraction, quantitatively. The 'minimum difference' refers to the

Table 2: Investigation of the difference between the results from our code and the KinFitter package. The effect of different algorithms is also compared. For definition of different abbreviations read the text.

| Algorithm | RecTop | Matched | purity | Eff | Imp $E_W$ Res | Imp $E_{Top}$ Res |
|---|---|---|---|---|---|---|
| minimum difference | 4117 | 443 | 11% | 16% | - | - |
| Partitioned Matrix | 3573 | 570 | 16% | 21% | - | - |
| Part Mat($\chi^2 < 9.2$) | 1279 | 341 | 27% | 12% | 38% | 53% |
| Fixed angles | 3524 | 588 | 17% | 21% | - | - |
| Fixed angles($\chi^2 < 9.2$) | 1282 | 342 | 27% | 12% | 38% | 53% |
| EtEtaPhi | 3643 | 661 | 18% | 24% | - | - |
| EtEtaPhi($\chi^2 < 9.2$) | 1358 | 374 | 28% | 14% | 42% | 59% |

mentioned test algorithm. 'RecTop' stands for the number of events for which the fit converges for at least one jet combination. In the case of 'minimum difference', this number shows the number of events with at least one W candidate (i.e., at lest 2 light jets) and one b-jet. 'Matched' refers to the number of the extracted top quarks

that are closer than $\Delta R = \sqrt{\Delta\eta^2 + \Delta\phi^2} = 0.5$ to a generated top quark that decays hadronically and all of its partons pass the kinematic cuts of the jets ($E_T \geq 30$ GeV and $|\eta| \leq 2.5$). The generated top quarks in an event with these features are referred to as *GenTopW*'s and will be used in next sections. The number of such generated top quarks in our sample is 3063 in 2767 events (some events have 2 or 3 top quarks). Since we select one top quark per event, to find the efficiency (shown in the table as 'Eff') the 'Matched' number is divided by 2767. The efficiency includes both the efficiency of the matching procedure and of the identification of the top quark. The 'purity' is defined as the percentage of the 'RecTop' that are 'Matched'. This is the purity against the combinatorial background. Other algorithms and parameters will be defined in next sections.

### 3.1.1 Impact of the fit on the kinematics of the reconstructed top

The main purpose of the kinematic fit is to reduce the combinatorial background and improve the jet selection for top quark (and W boson) reconstruction, as well as improve the kinematic features of the reconstructed objects. This expectation comes from the fact that the kinematic fit recovers partly the energy smearing of jets (by setting the mass scale).

The combination of jets with least $\chi^2$ is selected as the correct hypothesis provided its $\chi^2$ probability is greater than 0.01. To compare its features with a generated top quark, it is "matched" as defined in previous section. Figure 4 shows the result of the comparison between the energy resolution before and after the fit for both the top

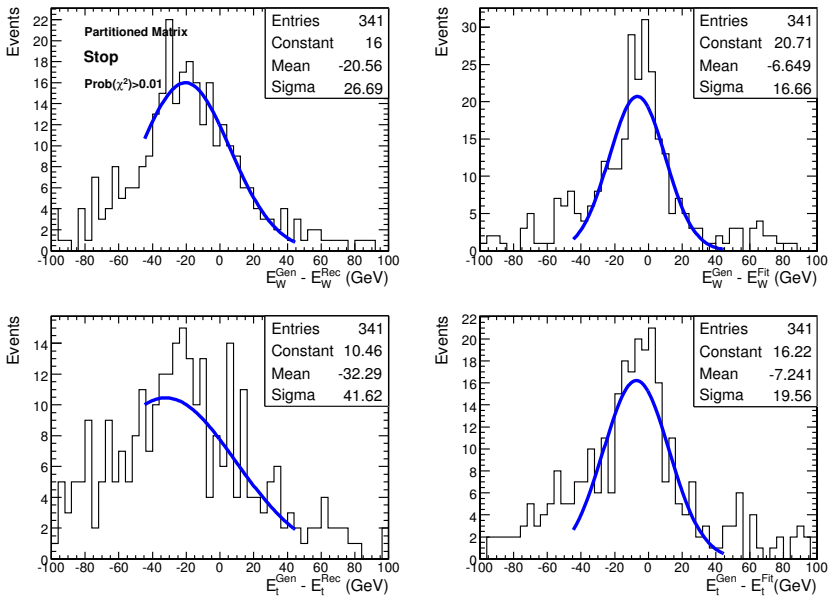


Figure 4: The difference between the energy of the reconstructed/fitted W(top) and the generated W(top). Fitted jet combinations pass the probability cut. The central parts of the distributions(-45,45) are fitted with a gaussian function (thick-blue lines) to emphasize and quantify the improvement in the resolution.

quark and W boson. It is clear that the fit has improved the energy resolution of both reconstructed objects. Table 2 summarizes this comparison for different algorithms. 'Imp $E_x$ Res' is the difference between the sigma of the gaussian fit to the central part of the distribution (-45, 45 GeV) before and after using the fit divided by the former value. The 'Partitioned Matrix', improves the resolution of the energy of the W and top quark by 38% and 53%, respectively. This large improvement of the top energy will be very important for the accuracy in reconstructing the stop mass in our future analysis.

## 3.2 The comparison with an existing package

The **KinFitter** package, adapted from the BaBar experiment [13] is a general package to perform a kinematic fit with constraints. In this package, one can parameterize a problem in different coordinate systems and jets can be massive. To have a fair comparison, the spherical coordinate system is selected and the jets are forced to be massless. The **KinFitter** program fits also the angles of the jets, which is not the case in the 'Partitioned Matrix'

formulation. To suppress this effect, the errors on angles are set to a very small value ($10^{-6}$). Table 2 compares the features of this algorithm with the other algorithms. This algorithm is referred to as 'Fixed angles'. The results are compatible with the ones from the 'Partitioned Matrix' method.

### 3.3 Fit including the jet angles

In **KinFitter** usually the objects are parameterized by energy and angles ($\theta$, $\phi$) and a free parameter that relates the energy to jet's momentum. In an experiment like CMS, usually massless jets are used and the parametrization is versus ($E_T$, $\eta$, $\phi$). We have added two classes to **KinFitter** to be able to handle this parametrization as well as an alternative parametrization using ($E_T$, $\theta$, $\phi$). Errors on angles are taken also from [14]. Table 2 compares the features of this algorithm (referred to as 'EtEtaPhi') with the others. The results are slightly better. It shows that the error on the direction of jets has no major effect compared to the error on the energy of jets. Hence our analysis is based on the simpler approach of partitioned matrices and allowing only energies of jets as variables.

### 3.4 The fit validation

Two important distributions to validate the performance of the fit are the $\chi^2$ probability distribution and the *PULL*-distributions. The PULL for every fitted parameter ($y_i$) is:

$$PULL(y_i) = \frac{y_{i,meas} - y_{i,fit}}{\sqrt{\sigma^2_{i,meas} - \sigma^2_{i,fit}}} \tag{2}$$

The $\chi^2$ probability distribution was shown in figure 3. The distribution has a peak at low probability. Such a peak is expected for events where the top hypothesis is wrong, but it could also reflect a problem with the uncertainties input or with the fit itself. To investigate this problem a fit was performed with the correct hypothesis. The kinematical quantities of the partons found in section 3.1, i.e., before the hadronization and fragmentation, are passed to the fit. To increase the statistics, we look at 100k events of $t\bar{t}$ sample which contains the inclusive decay of W's. Like before, the errors are the errors for the reconstructed jets. The result of the fit with the right hypothesis is shown in figure 5 (top thick-blue lines). It is clear that with the right hypothesis, the fit is convergent and the

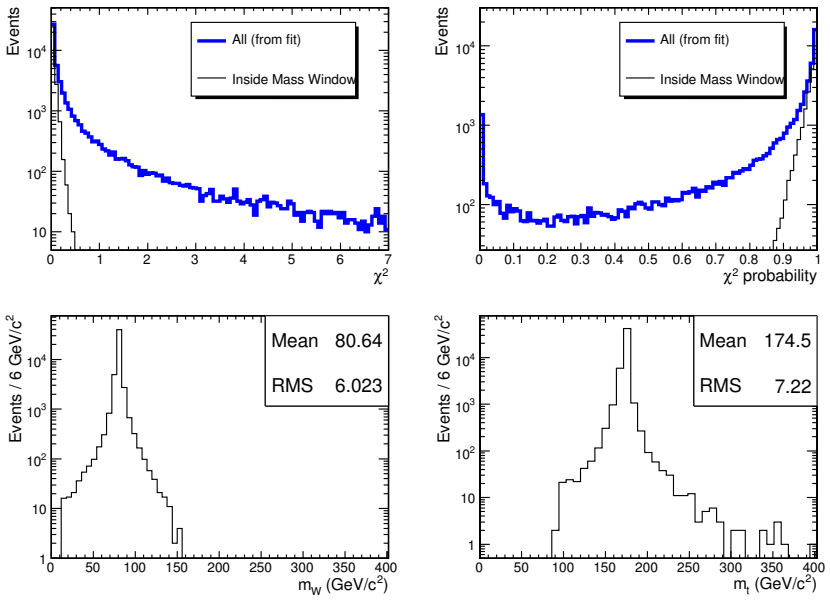


Figure 5: Distributions as in figure 3, starting from the right hypothesis (The generated partons from top quark). Starting from the right hypothesis with masses close to the nominal values give much better results (narrow-black line, see the text for more information).

value of $\chi^2$ is small (its probability distribution is skewed toward high values). The same distributions are also shown for parton combinations inside a mass window ($|m_{bjj} - 175| < 2.5$ and $|m_{jj} - 80| < 2.5$). It shows that

some of the low probability fits are due to the width of the W and top quark. The number of the used top quarks in this analysis is 50533 where 1356 (2.68 $\pm$ 0.07 % only statistical uncertainty) of them have $\chi^2$ probability less than 0.01.

To investigate the same problem after the hadronization and fragmentation the matched jets are used in the fit, but to avoid detector effects the stable particles at generator level are clusterized according to the jet finding algorithm used in the analysis. The closest jet, to each of the mentioned partons is found. If there are 3 distinct jets closer than $\Delta R = 0.2$ to the related generated partons from a top quark, the jets are used as the input of the fit. The number of these top quarks is 25090 where 2792 (11.13 $\pm$ 0.22 % only statistical uncertainty) of them are rejected after applying the cut of $\chi^2$ probability $> 0.01$. Figure 6 shows the $\chi^2$ and its probability distributions for the

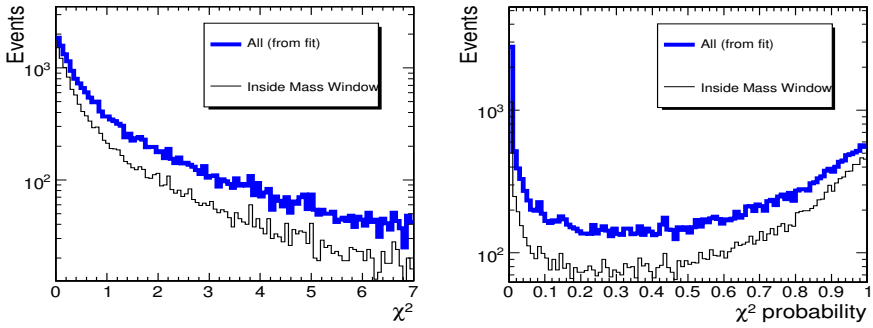


Figure 6: Distributions as in figure 5, starting from the clusterized stable particles, close to the generated partons from top quark. (see the text for more information)

mentioned jets. The $\chi^2$ distribution for the combinations with top and W inside the mass window shows two separately populated regions, the first one is in the high probability region that is similar to the corresponding peak in figure 5 (top-right) and shows the expected treatment of the correct hypotheses. The second peak is in the low probability region that shows the effect of the hadronization and fragmentation . In figure 5 (top-right) these combinations have a fit with a high $\chi^2$ probability, but when the hadronization and fragmentation is included and one parton can be correspond to more than one jet, these combinations may give a low probability fit.

The next step is to look at the reconstructed jets to see the detector effects. The same procedure as in the previous paragraph is used to match the jets to the partons. The number of the reconstructed top quarks is 9792. Applying the cut on the $\chi^2$ probability rejects 1494 (15.26 $\pm$ 0.42 % only statistical uncertainty) of the jet combinations. In figure 7 the same distributions as the previous figure are shown after using the new inputs. The comparison

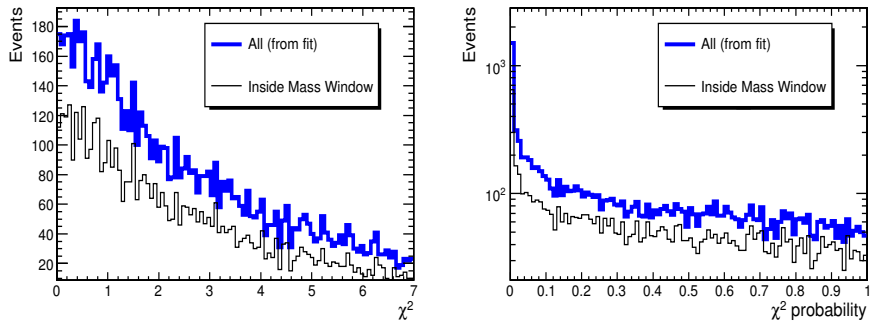


Figure 7: Distributions as in figure 6, starting from the reconstructed jets close to the generated partons from top quark. (see the text for more information)

between this figure and two previous figures and the efficiency of the cut on the $\chi^2$ probability shows that the main reason for the low probability fits is the hadronization and fragmentation. The detector effects contribution is less than the hadronization and fragmentation contribution. The detector effects can be improved in long term data taking after we have a better understanding of the jet calibration and error parametrization.

Other evidences for the goodness of the fit are the *PULL*-distributions. Figure 8 shows the *PULL*-distributions for the energies of the three jets, used in the fit (LM1-stop sample). The third jet is a b-tagged jet. In an ideal

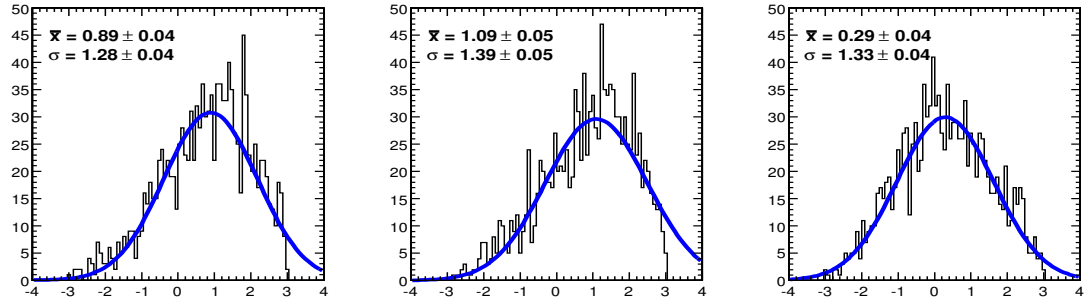


Figure 8: The *PULL*-distributions for the energy of different jets used in the fit. The third jet was chosen among the b-tagged jets. The $\chi^2$ probability with 2 degrees of freedom must be greater than 0.01. ($\chi^2 < 9.2$)

situation, a *PULL*-distribution must be gaussian with mean = 0, sigma = 1.0. In these distributions the $\sigma$'s are not consistent with one within the errors. It shows that the errors are underestimated. The shift in the mean values can be understood as overcorrection of jets by the 'GammaJet' algorithm. In figure 9 the *PULL*-distributions for the

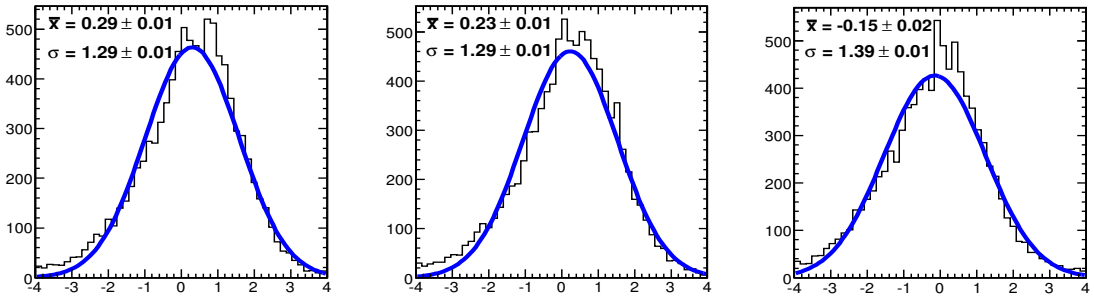


Figure 9: The *PULL*-distributions for the energy of different jets used in the fit in figure 7. The third jet is the closest jet to the b parton. Neither cut on $\chi^2$ probability nor mass are applied.

energy of the jets matched to the generated partons (jets used in figure 7) are shown. Comparing this figure with figure 8 indicates that the large shift in the central values of the *PULL*-distributions in the latter one is caused by the wrong combinations dominating the distributions (according to table 2 the purity is less than 1/3).

# 4 Sparticles Production and Decay in the Low Mass Point (LM1)

For illustration we use point CMS-LM1 ($B^{'}$ [2]) as benchmark point. mSUGRA is determined by 5 free parameters defined at the Grand Unification Theory (GUT) scale. The corresponding parameters for point LM1 are as follows: common scalar mass $m_0$ = 60 GeV/$c^2$, common gaugino mass $m_{1/2}$ = 250 GeV/$c^2$, common trilinear coupling $A_0$ = 0.0, the ratio of the vacuum expectation values of higgs fields $H_u$ and $H_d$, $\tan(\beta)$ = 10 and finally sign of the higgsino mixing parameter, sign($\mu$) = +1. Table 3 shows the masses of some important particles in point LM1. At

Table 3: Part of the spectrum in point LM1 generated by ISAJET7.69 [3]. $m_t$ is set to 175 GeV/$c^2$.

| Sparticle | Mass(GeV/$c^2$) | Sparticle | Mass(GeV/$c^2$) |
|---|---|---|---|
| $\tilde{u_R}$,$\tilde{c_R}$ | 541.52 | $\tilde{u_L}$,$\tilde{c_L}$ | 557.99 |
| $\tilde{d_R}$,$\tilde{s_R}$ | 541.18 | $\tilde{d_L}$,$\tilde{s_L}$ | 563.99 |
| $\tilde{b_2}$ | 534.96 | $\tilde{b_1}$ | 514.17 |
| $\tilde{t_2}$ | 575.85 | $\tilde{t_1}$ | 411.91 |
| $\tilde{g}$ | 611.32 | $\chi_2^{\pm}$ | 360.99 |
| $\chi_1^{\pm}$ | 179.50 | $\chi_4^0$ | 361.81 |
| $\chi_3^0$ | 341.29 | $\chi_2^0$ | 179.56 |
| $\chi_1^0$ | 94.93 | $h_0$ | 112.87 |

this point the top can be generated indirectly in the decay of heavier sparticles (gluino, stops and sbottoms have a chance to decay to top). The cross section for the inclusive production of top in point LM1 is 6.787 pb (LO, PYTHIA [4] (NLO, PROSPINO [15] >9 pb)), whilst the inclusive SUSY production cross section is 42 pb (LO, PYTHIA (NLO, PROSPINO 52 pb)). Table 4 shows the branching ratios for all possible decays to top. The SUSY

Table 4: The relevant branching ratios in point LM1 generated by PYTHIA 6.225. The numbers for gluino decays include the charge conjugate decays also. $\chi^0_{all}$ means all neutralinos.

| $Mother \rightarrow Daughters$ | B.R(%) | $Mother \rightarrow Daughters$ | B.R(%) |
|---|---|---|---|
| $\tilde{g} \rightarrow \bar{t} + \tilde{t_1}$ | 6.16 | $\tilde{g} \rightarrow \bar{b} + \tilde{b_1}$ | 18.09 |
| $\tilde{g} \rightarrow \bar{b} + \tilde{b_2}$ | 12.67 | $\tilde{t_2} \rightarrow Z^0 + \tilde{t_1}$ | 12.17 |
| $\tilde{t_2} \rightarrow h_0 + \tilde{t_1}$ | 2.62 | $\tilde{b_2} \rightarrow W^- + \tilde{t_1}$ | 16.33 |
| $\tilde{b_1} \rightarrow W^- + \tilde{t_1}$ | 6.64 | $\tilde{t_1} \rightarrow \chi^0_2 + t$ | 12.53 |
| $\tilde{t_1} \rightarrow \chi^0_1 + t$ | 17.70 | $\tilde{t_2} \rightarrow \chi^0_{all} + t$ | 40.58 |
| $\tilde{b_1} \rightarrow \chi^+_1 + t$ | 48.36 | $\tilde{b_2} \rightarrow \chi^+_1 + t$ | 23.85 |

sample was generated by PYTHIA which computes only LO cross sections. For simplicity the whole sample is scaled to the NLO cross section without changing the proportion for different channels. This assumption leads to an underestimation of signal events, because taking into account the NLO cross section increases the signal with respect to the rest of the SUSY channels, significantly (Table 5).

Table 5: Cross sections in (pb) from different programs. The first two columns are the results of PROSPINO. These are the channels that participate in the signal production (direct sbottom production is not included). It can be seen that the K-factor is almost 1.5, but the K-factor for inclusive SUSY is only ($\frac{52}{42} \approx$) 1.24, so our assumption to scale the whole SUSY sample is on the safe side and leads to a conservative result.

| | LO | NLO | Isa-Pythtia |
|---|---|---|---|
| $\tilde{t_1}\tilde{t_1}$ | 1.351±.0016 | 2.149 ± .0037 | 1.09 |
| $\tilde{q}\tilde{g}$ | 22.14± .0016 | 29.74± .0031 | 20.06 |
| $\tilde{g}\tilde{g}$ | 6.499±.0017 | 10.58 ± .0024 | 4.573 |

# 5 The Data Samples

The samples used in this analysis and their cross sections are shown in Table 6. The multi jets and $W + jets$

Table 6: Cross sections for important samples.

| Sample | LO | NLO |
|---|---|---|
| ZW | 26.89 | 51.5 |
| WW | 188.1 | 269.91 |
| $t\bar{t}$ | 492.2 | 830 |
| single top | - | 250 |
| SUSY LM1 | 42.07 | 52 |

samples are listed in tables 8 and 9, respectively. All samples are the officially produced samples listed in Reference [16]. The SUSY sample was generated using the ISAJET 7.69 [3] interfaced with PYTHIA 6.225 [4] package. The events were simulated using OSCAR_3_6_0 [6], digitized with low luminosity pileup and reconstructed with ORCA_8_7_1 [7]. The production chain is exactly the same for SM samples, starting from PYTHIA. The single top sample (containing only the t-channel production) and $W + bb$ (Table 9) were generated by using TopReX 4.11 [17]. Apart from the $W + jets$ sample, all SM samples include both hadronic and leptonic decay of W. The SUSY sample is also inclusive and contains all allowed productions and decays corresponding to their leading order (LO) cross sections and branching ratios. For Next-to-Leading-Order (NLO) cross sections, the official values in CMS are used. WW is a mixture of vector boson fusion (EW process with K-factor close to one) and $q\bar{q}$ fusion. We use the K-factor of the second part ($\sim$ 1.5) for whole sample. It leads to overestimating the contribution of this sample, but it will be shown that these events can be rejected completely.

# 6 Analysis Path

In this note our strategy to search for SUSY is to look at the number of extracted top quarks for 1 $fb^{-1}$. In the following, SUSY events are divided in two parts, SUSY(withTop), SUSY events with a generated top quark and SUSY(noTop), SUSY events without a top quark at the generator level. This separation allows to optimize the cuts to suppress the second part as the fake signal. Different cuts and selections used in this analysis are as follows:

**L1T** In the first level of trigger, every event has to satisfy the thresholds for the Jet/Met trigger [8]. The trigger consists of a logical AND between a central jet and MET with the thresholds of 88 and 46 GeV, respectively.

**HLT** Every event is required to pass the Jet/Met conditions of the High Level Trigger (HLT). This trigger consists of a logical AND between a single jet and MET with the thresholds of 180 and 123 GeV, respectively.

**MET $>$ 150GeV** The most important background is the inclusive $t\bar{t}$, because it has a very high cross section (830 pb) and it has two real top quarks per event. SUSY events have at least two $\chi_1^0$, appearing as missing transverse momentum (MET), but MET in $t\bar{t}$ events comes from neutrinos or mis-measurements and usually does not exceed a few 10 GeV. Figure 10 compares the MET distributions from different samples. To

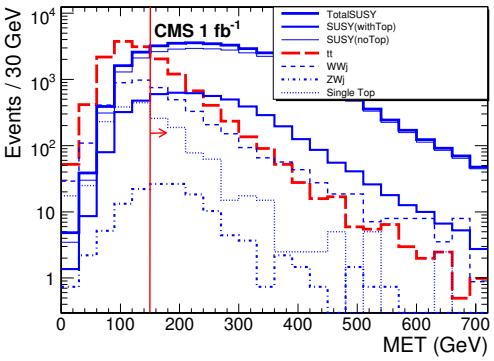


Figure 10: MET distributions for different samples. Every event is asked to pass L1T and HLT.

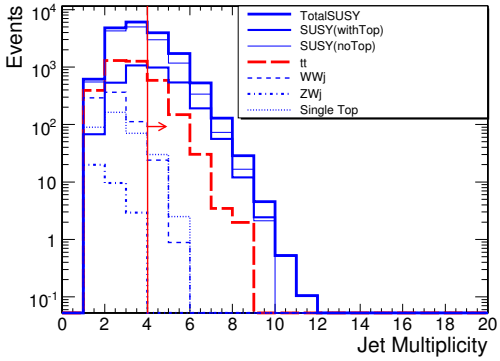


Figure 11: The jet-multiplicity in the events that pass the cut on MET. The distribution contains the both light jets and b-jets with $E_T^{Raw} \geq 30$ GeV.

increase the ratio of the SUSY events to $t\bar{t}$ and other SM backgrounds, a cut on MET is introduced (MET $\geq$ 150 GeV).

**at least 1 b-jet** The top quark almost always decays to a b-jet plus a W, so in every event at least one jet must be tagged as a b-jet.

**at least 4 jets** We are looking for a hadronically decaying top candidate, so every event must have at least two light jets apart from the b-jets. Figure 11 shows the jet multiplicity distribution in this step. The events with less than 4 jets are rejected to suppress the SM background. Since later we would like to use the fast simulation (FAMOS [18]) to perform the scan in $m_0 - m_{1/2}$ plane, the cut on $E_T$ of the jets is changed to only $E_T^{Raw} \geq 30$ GeV. With this cut the results from ORCA and FAMOS are more consistent. Moreover, this cut is less sensitive to the jet energy scale systematics.

**a convergent fit with a $\chi^2$ probability $>$ 0.1** To find a top quark, the best jet combination is found by the kinematic fit. A cut on the $\chi^2$ probability is applied to increase the purity of the selected top quarks. Figure 12 shows the distribution of the $\chi^2$ probability for the extracted top quarks in different samples. It will be shown that this cut significantly removes non-TOP background (e.g. multi-jets and W+jets).

**$\Delta\phi$ between the fitted top and MET $<$ 2.6 rad** Since we look for a hadronically decaying top quark in the events with a large MET, mostly semileptonic $t\bar{t}$ events can mimic the signal. In these events, MET is from one side and the reconstructed top is from the other side and in the transverse plane they are close to back-to-back. Figure 13 shows the $\Delta\phi$ between the fitted top quark (the energy of the jets have been changed by the fit which affects the direction of top) and MET in SUSY and $t\bar{t}$ events. Applying a cut on this parameter, $\Delta\phi <$ 2.6, suppresses efficiently the $t\bar{t}$ events.

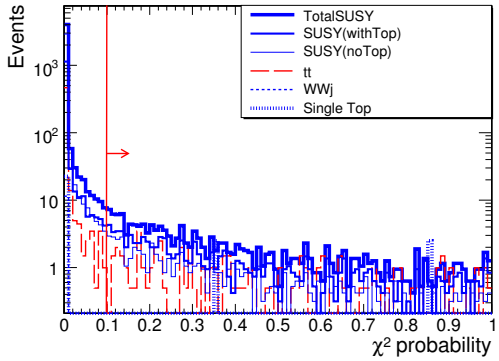


Figure 12: $\chi^2$ probability distributions for different samples. Every event passes the cuts on HLT and jet multiplicity and has a convergent fit. SUSY(withTop) and SUSY(noTop) are concentrated in different regions.

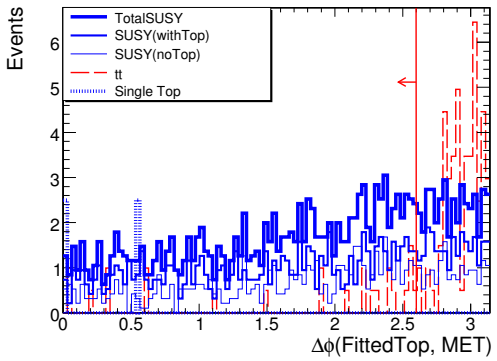


Figure 13: The $\Delta\phi$ between the fitted top quark and MET in events that pass the cut on the $\chi^2$ probability. To suppress the remaining $t\bar{t}$ background a cut on this parameter is applied.

Table 7 shows the number of remaining events after every cut. In this table SUSY events are divided in two parts,

Table 7: Effect of different cuts on different samples. In every row, the number of the remaining events after that cut is shown. "No.of.used.events" shows the number of events used in this analysis, "NEve(Nor.xsec)1 $fb^{-1}$" is the same number after normalizing to the cross section times 1 $fb^{-1}$ and "wT/noT" means $\frac{SUSY(withTop)}{SUSY(noTop)}$.

| cut | SUSY(withTop) | SUSY(noTop) | $t\bar{t}$ | WW | ZW | Single Top | wT/noT |
|---|---|---|---|---|---|---|---|
| x-sec(pb) NLO | 52 | | 830 | 269.91 | 51.5 | 250 | - |
| No.of.used.events | 494261 | | 1674500 | 305000 | 70000 | 100000 | - |
| NEve(Nor.xsec)1 $fb^{-1}$ | 8375 | 43625 | 830000 | 269910 | 51500 | 250000 | 0.19 |
| L1T (Jet/Met) | 6269 | 33582 | 75806 | 18498 | 598 | 10875 | 0.19 |
| HLT (Jet/Met) | 5070 | 29427 | 14430 | 4733 | 142 | 1750 | 0.17 |
| MET$\geq$ 150 GeV | 4183 | 25677 | 4930 | 2312 | 99 | 653 | 0.16 |
| $n_{bj} \geq 1$ | 3457 | 14388 | 3718 | 792 | 32 | 355 | 0.24 |
| $n_j^{b\ or\ light} \geq 4$ | 1789 | 4576 | 769 | 25 | 0 | 33 | 0.39 |
| A convergent Fit | 1335 | 3062 | 557 | 12 | 0 | 28 | 0.44 |
| $\chi^2$ probability >0.1 | 105 | 69 | 56 | 0 | 0 | 5 | 1.52 |
| $\Delta\phi$ <2.6 | 79 | 52 | 12 | 0 | 0 | 5 | 1.51 |
| $n_l > 0$ | 38 | 17 | 5 | 0 | 0 | 0 | 2.19 |

"SUSY(withTop)" and "SUSY(noTop)". Although, the sum of both parts is used as the number of signal events (S), we try to increase the ratio of the first part as the real signal against the second part. Asking for a convergent fit and applying the cut on the $\chi^2$ probability $> 0.1$, increases the ratio of the real top quarks in SUSY events. This can be understood in the sense that $\chi^2$ probability quantifies the goodness of a reconstructed top quark, so fake top quarks are fitted with a smaller $\chi^2$ probability. Table 8 shows the effect of the cuts on the multi jets backgrounds. It can be seen that the former cuts are not sufficient to suppress these backgrounds.

**at least one isolated lepton** To suppress the multi jets backgrounds, events are asked to have at least one isolated electron or muon with $P_T > 5$ GeV/c and $|\eta| < 2.5$. There should not be any jet closer than $\Delta R = 0.2$ to a lepton. This requirement can suppress the muons coming from the b-jets.

Table 9 summarizes the specifications of $W + jets$ samples and the effect of the cuts on them. It can be seen that the cuts suppress the contribution of these samples effectively, although the number of used events are limited. Also from the Table 7 the same result can be concluded. WW is an inclusive sample and can be considered as $W+ > 2\ jets$ in our analysis. It can be seen that all events are suppressed after applying the cut on the $\chi^2$

Table 8: The multi jets backgrounds. $\hat{P_T}$ is the $P_T$ of the generated partons. In every column the number of remaining events after that cut is shown. Note that in this table, real numbers are shown, although in tabel 7 numbers are scaled to 1 $fb^{-1}$. "No.Used" shows the number of events used in the analysis.

| $\hat{P_T}$ range | x-sec(pb) | No.Used | L1T | HLT | MET | $n_{bj}$ | $n_j$ | $\chi^2$ | $\Delta\phi$ | $n_l$ |
|---|---|---|---|---|---|---|---|---|---|---|
| 80-120 | 3.0e+6 | 242486 | 874 | 0 | 0 | 0 | 0 | 0 | 0 | 0 |
| 120-170 | 5.0e+5 | 213842 | 9189 | 29 | 1 | 0 | 0 | 0 | 0 | 0 |
| 170-230 | 1.0e+5 | 338478 | 48009 | 495 | 12 | 3 | 0 | 0 | 0 | 0 |
| 230-300 | 23800 | 389978 | 108256 | 1866 | 78 | 42 | 2 | 0 | 0 | 0 |
| 300-380 | 6400 | 283983 | 114690 | 2984 | 241 | 152 | 22 | 0 | 0 | 0 |
| 380-470 | 1880 | 191989 | 97488 | 4056 | 466 | 350 | 40 | 1 | 1 | 0 |
| 470-600 | 690 | 175987 | 104025 | 6759 | 905 | 740 | 156 | 0 | 0 | 0 |
| 600-800 | 202 | 94957 | 64547 | 6758 | 1031 | 907 | 222 | 0 | 0 | 0 |
| 800-1000 | 35.7 | 49499 | 38539 | 5602 | 976 | 908 | 262 | 1 | 1 | 0 |
| 1000-1400 | 10.8 | 23250 | 19869 | 3761 | 841 | 812 | 269 | 0 | 0 | 0 |
| 1400-1800 | 1.06 | 2700 | 2476 | 570 | 155 | 145 | 57 | 1 | 1 | 0 |

probability. (Note that the scale factor for this sample is less than 1.)

Table 9: $W + jets$ samples. The definitions are same as in Table 8. Although some samples suffer from the low population, the robustness of the cuts against these backgrounds is visible.

| sample | x-sec(pb) | No.Used | L1T | HLT | MET | $n_{bj}$ | $n_j$ | $\chi^2$ | $\Delta\phi$ | $n_l$ |
|---|---|---|---|---|---|---|---|---|---|---|
| Wbb | 106.59 (LO) | 224000 | 1437 | 593 | 349 | 271 | 1 | 0 | 0 | 0 |
| Wj 25$< \hat{P_T} <$170 | 10069 (LO) | 757936 | 6057 | 423 | 67 | 9 | 0 | 0 | 0 | 0 |
| Wj 200$< \hat{P_T} <$1400 | 48.86(LO) | 86000 | 55203 | 39839 | 25376 | 7142 | 124 | 3 | 0 | 0 |

To optimize the cuts each of them was varied separately leading to the values presented in table 7. These cuts were optimized to increase $\frac{SUSY(withTop)}{SUSY(noTop)}$ and decrease the SM background simultaneously, whilst keeping the significance sufficiently high. The significance is defined as follows [19]:

$$Significance = 2 \times (\sqrt{S+B} - \sqrt{B}) \tag{3}$$

where $S$ and $B$ are the number of the remaining events after all cuts for the signal and background, respectively.

# 7 Systematic Uncertainties

Here we only consider the systematic uncertainties for the $t\bar{t}$ sample. For the Jet Energy Scale (JES), we follow the recommendation of the CMS Jet/Met group [20]. Assuming 5% uncertainty for the jet absolute energy scale in 1 $fb^{-1}$, the energy of jets was scaled by $(1 \pm 0.05)$. The difference between the maximum and minimum number of remaining $t\bar{t}$ events was found, $(|\Delta^+ - \Delta^-|)$, half of this value, normalized to the reference value is used as the relative systematic uncertainty for this cut. To avoid the statistical uncertainty on this value the cut on HLT and MET are relaxed to increase the number of the remaining events. The resulting relative systematics from JES is 5.1%. To evaluate the effect of JES on MET, its value was scaled to $(1 \pm 0.05)$ and the same procedure as the previous step was repeated. In this step the cuts on L1T, HLT, $n_j^{b\ or\ light} \geq 4$, $\Delta\phi < 2.6$ and $n_l > 0$ were relaxed to have a reasonable statistics (more than 500 real events corresponding to ∼250 events for 1 $fb^{-1}$). The resulting relative systematics from JES on MET is 18.3%. For b-tagging, the reported uncertainty by the b-tau group [20] is used (8% uncertainty for 1 $fb^{-1}$). We will consider here only the JES and b-tagging uncertainty to be relevant. The rest of the systematics (cross section, showering, ISR/FSR,...) will be eliminated or rendered very small by using the real data. For example low $P_T$, high statistics samples prescaled at the trigger level can be used to extrapolate to the high missing energy region. The systematic uncertainties from the JES and b-tagging are added quadratically and the result is a total systematic uncertainty of 20.6%. One can decrease the cut on the $\chi^2$ probability to increase the efficiency, but it would increase the systematic uncertainties. To investigate the problem and quantify it, different values are tried and for every value the relative uncertainty from JES uncertainty on jets is evaluated. The results are shown in table 10. It can be seen that $\chi^2$ probability $> 0.10$ corresponds to the lowest systematic uncertainty.

Table 10: The effect of different cut on $\chi^2$ probability. The used value (0.1) is optimized to decrease the systematic uncertainties.

| cut value | S/B | SUSY(wTop/noT) | Total SUSY | uncertainty from JES |
|---|---|---|---|---|
| 0.01 | 10 | 1.7 | 112 | 8.5 % |
| 0.05 | 12 | 1.9 | 73 | 7.3 % |
| 0.10 | 11 | 2.2 | 55 | 5.1 % |
| 0.15 | 9.2 | 2.3 | 46 | 6.3 % |

# 8 Results

The number of events remaining after all cuts are summarized in table 11. In the events extracted as signal, $\frac{38}{38+17} = 69\%$ are from SUSY events which have a top quark at the generator level. The efficiencies for the different samples are also listed in table 11. Figure 14 shows the MET distribution after applying all cuts. The

Table 11: Number of the remaining events after all cuts for 1 $fb^{-1}$. The overall efficiency for different samples is shown in the last column. The efficiencies for the QCD and $W + jets$ are not shown due to the lack of the statistics.

| sample | No.remaining.events | efficiency |
|---|---|---|
| SUSY(withTop) | 38 | 4.5e-3 |
| SUSY(noTop) | 17 | 3.9e-4 |
| $t\bar{t}$ | 5 | 6.0e-6 |
| WW | 0 | <3.2e-6 |
| ZW | 0 | <1.4e-5 |
| single top | 0 | <1.0e-5 |
| multi jets | 0 | - |
| W+jets | 0 | - |

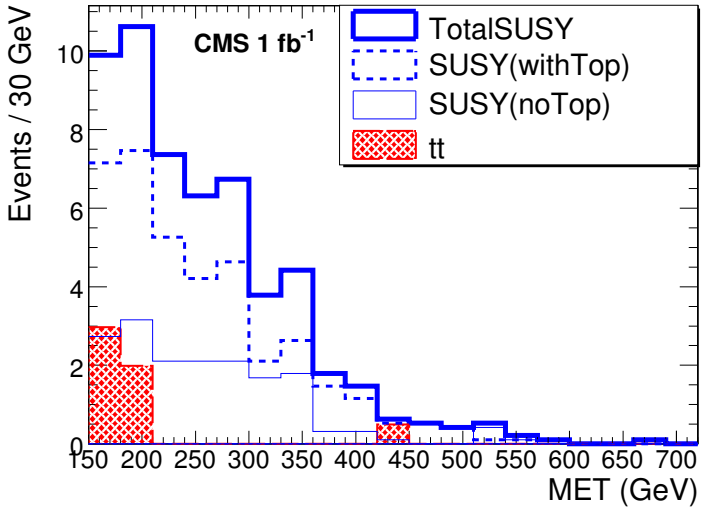


Figure 14: MET distribution after all cuts.

SUSY signal is significantly higher than the SM ($t\bar{t}$) background, although the shapes are similar. One can cut on a higher MET value to suppress completely the $t\bar{t}$ background, but to avoid the large uncertainty on the tail of the MET distribution the cut is left low. Figure 15 shows the invariant mass distribution for the extracted W and top quark in different samples after all cuts. It is clear that $t\bar{t}$ is sufficiently suppressed.

We try to find the minimum integrated luminosity to achieve a 5 $\sigma$ discovery. The significance corresponding to equation (3) varies with the square root of the integrated luminosity. Using $S$ and $B$ for 1 $fb^{-1}$, the minimum

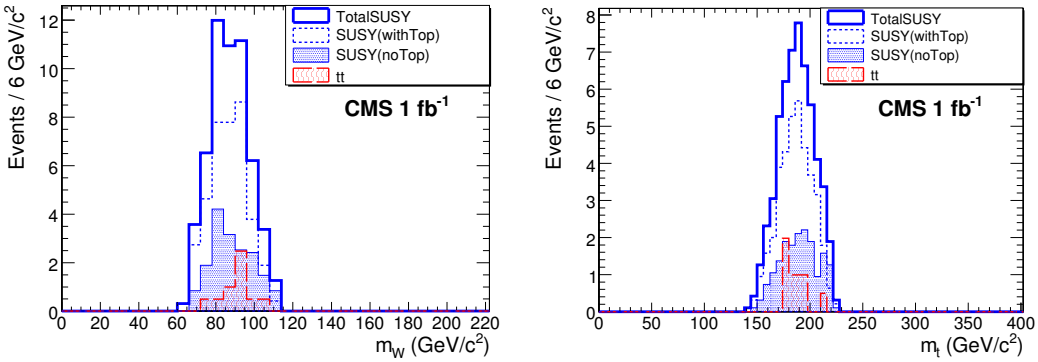


Figure 15: dijet (W) and bjj (top) invariant mass distributions for different samples after applying all cuts.

integrated luminosity can be found by solving the equation:

$$5 = \sqrt{\alpha} \times 2 \times (\sqrt{(38+17)+(5)} - \sqrt{5}) \Rightarrow \alpha = 0.21 fb^{-1} \quad (4)$$

For this integrated luminosity, the corresponding number of events for signal and background are 11 and 1 , leading to 100% statistical uncertainty on the background which is larger than the systematics uncertainty, so the latter one can be neglected. Including the systematic uncertainties by the proper algorithm implemented in a program [21] leads to 0.25 $fb^{-1}$ as the minimum integrated luminosity to achieve a 5 $\sigma$ discovery. Note that the analysis uses b-tagging and systematics that are realizable with 1 $fb^{-1}$. For start-up (0.1 $fb^{-1}$) a separate study needs to be performed.

It is seen in table 4 that the channels which dominate the signal production ($\tilde{g}$ and $\tilde{t_1}$ production), always contain another b-jet. It can be shown that asking for two b-jets is powerful against the W+n$j$ and multi jets backgrounds. By knowing the b-tagging accurately, one can require at least two b-jets, but this would need higher integrated luminosity. Moreover, here we have used top+MET as an indicator for SUSY, although other indicators like top + number of jets, $P_T$ of top etc, also can be used, but are beyond the scope of this note and will be considered in future studies.

# 9 CMS Reach in $m_0$-$m_{1/2}$ Plane

In this section the same cuts are applied on SUSY samples generated in different points of the allowed region of the parameter space to determine the reach of the CMS experiment. To speed up the analysis, the fast simulation and reconstruction of CMS, FAMOS [18], is used. Also events are analyzed without adding the effect of the pileup. For the SUSY events, this has a negligible effect. To find the reach of the CMS experiment in the mSUGRA space, only the $m_0$ and $m_{1/2}$ are changed and the other parameters are fixed equal to their corresponding values for LM1. In total 36 points in $m_0$-$m_{1/2}$ plane are tested. In every point at least 10000 events are generated using PYTHIA linked to ISAJET. The generated ntuples are used as the input for FAMOS. After applying the cuts, the number of remaining events is divided by 1.3 to compensate the higher efficiency of FAMOS with respect to the full simulation observed at point LM1 and the $t\bar{t}$ background. The extracted number is normalized to the NLO cross section and the corresponding number of events for 1 $fb^{-1}$ is found. The NLO cross section is calculated by PROSPINO, assuming only the $\tilde{g}-\tilde{g}$, $\tilde{g}-\tilde{q}$ and $\tilde{q}-\tilde{q}$ productions to be relevant. The minimum signal over background is as high as 40%. The same method as used in the previous analysis is applied to find the minimum integrated luminosity for a 5$\sigma$ discovery. To find the curves corresponding to reach for 1, 10 and 30 $fb^{-1}$, the minimum integrated luminosity in neighbouring points is extrapolated linearly. The result is shown in figure 16. The larger reach in the high $m_0$ region can be understood as follows. The gluino mass is independent of $m_0$ so the isomass curves for the gluino are almost horizontal. It leads to an almost $m_0$-independent cross section for $\tilde{g}-\tilde{g}$ production. But squarks and then stop become heavier than the gluino when for constant $m_{1/2}$, $m_0$ is increased. In the high $m_0$ region, gluino is not kinematically allowed to decay to the squarks or stop, so the three body decays of gluino to chargino + $q\bar{q'}$ and neutralino + $q\bar{q}$ are dominant. The branching ratio to the final states containing a top quark can be as high as 40% leading to a large cross section $\times$ branching ratio for the top quark production in this region. Figure 17 shows the CMS reach after including the systematic uncertainties. For 10 and 30 $fb^{-1}$, the jet energy scale uncertainty is taken to be 3% [20] for both jets and MET. The same procedure as what was explained in section 7 is used to find the relative systematic uncertainties for these integrated luminosities. The relative systematic uncertainty from JES on jets is 3.1% and on MET is 11.3%. The relative systematic uncertainty

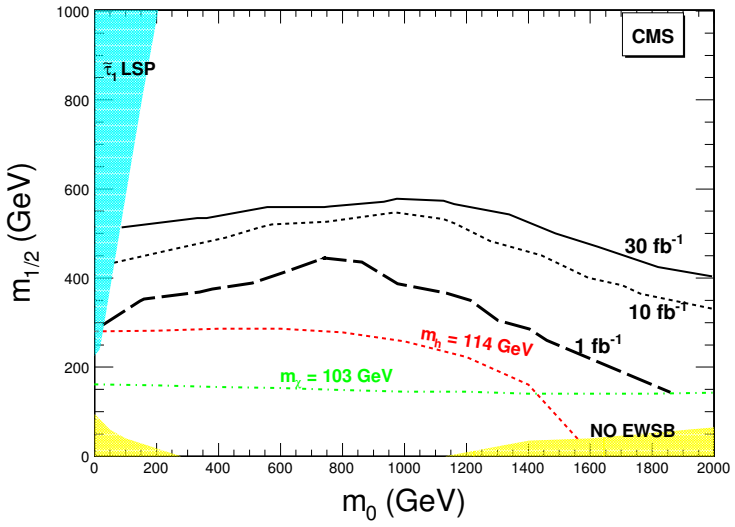


Figure 16: The CMS experiment reach for mSUGRA in top+MET final states in $m_0$-$m_{1/2}$ plane. Different exclusions from theory and experiment are also shown.

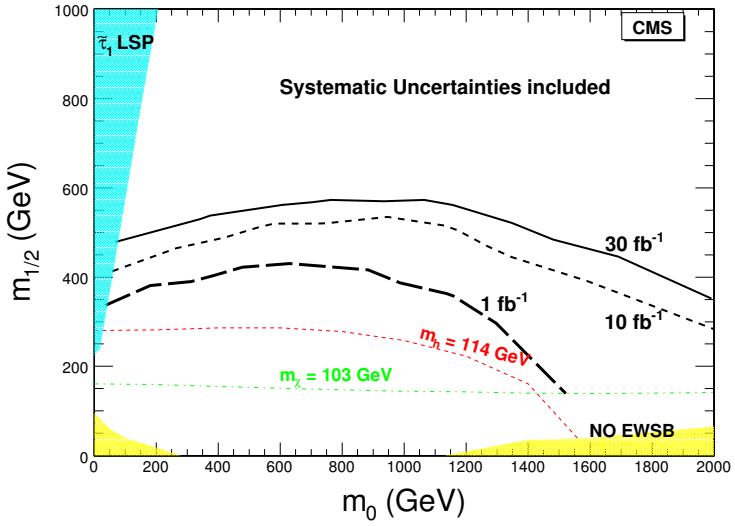


Figure 17: Same as figure 16 after including the systematic uncertainties.

from the b-tagging is 7% [20]. The total relative systematic uncertainty which is the quadratic sum of the previous ones is 13.7%. Thanks to the sufficiently high S/B, the effect of the systematic uncertainties is minor.

# 10 Conclusion

The capability of CMS to find low mass SUSY in events with a top quark in the final state was studied. A two constraint kinematic fit was utilized to improve the top quark extraction. It is shown that for point LM1 with an integrated luminosity of 0.2 $fb^{-1}$, a 5 $\sigma$ discovery is achievable provided the uncertainty is statistics dominated. The final signal over background ratio is 11.0. The CMS reach contours for 1, 10 and 30 $fb^{-1}$ are presented by using the fast simulation of the detector response, checked against the full simulation. The presented analysis method will allow to study in detail the kinematic properties of the stop (or other involved sparticles) decays.

# 11 Acknowledgment

The authors would like to thank the referees of the analysis, Oliver Buchmüller and Michael Schmitt for spending time to read the text and raise useful comments. Special thanks to Oliver Buchmüller for his fruitful discussions to improve the kinematic fit code. This work was done by using the CMS collaboration developed softwares, so many thanks to CMS software people, specially Stephan Wynhoff and ORCA developers, Tony Wildish and production team, Ian Fisk and CRAB team both at CERN and FNAL. Also thanks to Nicola Amapane, Emilio Meschi, Salavat Abdoulline and Filip Moortgat for their help and suggestions. S.P would like to thank Reyes Alemany Fernandez: the same work for Jet/Lepton separation was done at the generator level using FAMOS with her help.

# References

[1] Stephen P. Martin, "A Supersymmetry Primer", (hep-ph/9709356 v3 7 Apr 1999).

[2] M.Battaglia et al. Eur.Phys.J. C33 (2004) 273-296, [arXiv:hep-ph/0306219].

[3] http://www.phy.bnl.gov/∼isajet/

[4] T. Sjöstrand, P. Edén, C. Friberg, L. Lönnblad, G. Miu, S. Mrenna and E. Norrbin, Computer Phys. Commun. 135 (2001) 238 (LU TP 00-30, hep-ph/0010017)

[5] CMS Coll, http://cmsdoc.cern.ch/cmsoo/projects/CMKIN/

[6] CMS Coll, Object oriented Simulation for CMS Analysis and Reconstruction http://cmsdoc.cern.ch/oscar/

[7] CMS Coll., Object oriented Reconstruction for CMS Analysis, http://cmsdoc.cern.ch/orca/

[8] CMS Coll., "The Trigger and Data Acquisition project,Volume II",CERN/LHCC 2002-26,CMS TDR 6.2,15 December 2002.

[9] A.-S. Giolo-Nicollerat, "Electron reconstruction and electroweak processes as tools to achieve precision measurements at a hadron collider: from CDF to CMS", CERN-THESIS-2005-042.

[10] V. Konoplianov, A. Ulyanov, O. Kodolova, "Jet Calibration using $\gamma$+Jet Events in the CMS Detector", CMS NOTE 2006/042.

[11] Lj. Simić et al. ATL-PHYS-2002-009

[12] R.K. Bock, "Application of a generalized method of least squares for kinematical analysis of tracks in bubble chambers", CERN. Geneva, 1960.- CERN-60-30. R.K. Bock, "Kinematic analysis of bubble chamber events: FIT : an IBM 709 programme imposing momentum and energy conservation on measurements of complete events", CERN. Geneva, 1961.-CERN-61-29. R.K. Bock, "Formulae and methods in experimental data evaluation, with emphasis on high energy physics v.3 : Articles on statistical and numerical methods", CERN. Geneva, 1983.

[13] J. D'Hondt et al. "Fitting of Event Topologies with External Kinematic Constraints in CMS", CMS NOTE 2006/023.

[14] A. Heister et al. "Jet Reconstruction and Performance in the CMS Detector", CMS Note 2006/036.

[15] W.Beenakker, R.Hoepker, M.Spira, "PROSPINO: A Program for the Production of Supersymmetric Particles in Next-to-leading Order QCD", hep-ph/9611232.

[16] http://cmsdoc.cern.ch/cms/production/www/html/general/index.html

[17] S. R. Slabospitsky, L. Sonnenschein, Comput. Phys. Commun. 148 (2002) 87, hep-ph/0201292 http://sirius.ihep.su/∼spitsky/toprex/toprex.html

[18] http://cmsdoc.cern.ch/famos/

[19] S.I. Bityukov, N.V. Krasnikov, "On observability of signal over background", NIM A 452: 518-524, 2000.

[20] CMS Coll., "CMS Physics Technical Design Report, Volume I, Detector Performance and Software", CERN/LHCC 2006-001, CMS TDR 8.1, 2 February 2006.

[21] S.I. Bityukov, S.E. Erofeeva, N.V. Krasnikov, A.N. Nikitenko, Conference Proceedings of PHYSTAT2005: Statistical Problems in Particle Physics, Astrophysics, and Cosmology, Editors: Louis Lyons, Muge Karagoz Unel, Imperial College Press, 2006.